ISSN 1990-7931, Russian Journal of Physical Chemistry B, 2012, Vol. 6, No. 2, pp. 276–288. © Pleiades Publishing, Ltd., 2012.
Original Russian Text © S.M. Frolov, A.V. Dubrovskii, V.S. Ivanov, 2012, published in Khimicheskaya Fizika, 2012, Vol. 31, No. 3, pp. 32–45.

COMBUSTION, EXPLOSION, AND SHOCK WAVES

Three-Dimensional Numerical Simulation of the Operation of the Rotating-Detonation Chamber

S. M. Frolov, A. V. Dubrovskii, and V. S. Ivanov

Semenov Institute of Chemical Physics, Russian Academy of Sciences, Moscow, Russia

e-mail: smfrol@chph.ras.ru

Received August 19, 2011

Abstract—The aim of this work is to apply three-dimensional numerical simulation to determining the conditions of the stable operation of the rotating-detonation chamber (RDC), the thermal state of the chamber walls, as well as the most important parameters of the flow at the inlet and outlet, keeping in mind the possibility of placing the RDC between a compressor and a turbine in a prospective gas turbine installation. The model is based on a system of three-dimensional unsteady Reynolds-averaged Navier–Stokes, energy, and species conservation equations for a multicomponent reacting gas mixture supplemented by a turbulence model. The system is solved using a combined algorithm based on the finite-volume and particle methods. The capabilities of the computer program are demonstrated by the example of a circular RDC with inner and outer walls 260 and 306 mm in diameter and with axial introduction of a hydrogen–air mixture through an annular gap at the bottom of the chamber (with a relative area of 0.6). The detonation wave spun over the bottom at a frequency of ~126000 rpm. Calculations have shown that such an RDC can operate in a steady mode with one detonation wave.

Keywords: rotating-detonation chamber, numerical simulation, region of existence of detonation.

DOI: 10.1134/S1990793112010071

INTRODUCTION

A rotating-detonation jet engine, first proposed by Voitsekhovsky in 1959 [1], is considered one of the most promising for further improving the aircraft propulsion units and power plants, in particular, gas turbine installations (GTI).

To understand how the rotating-detonation chamber (RDC) operates, consider an annular channel formed by the walls of two coaxial cylinders of equal length. Mounting a nozzle head at the bottom of the cylinders to provide supply of fuel components into the annular channel and a jet nozzle at the other end of the channel makes an annular flow reactor. Combustion in such a reactor can be realized in different ways: either as in an ordinary liquid rocket engine (LRE) or according to Voitsekhovsky's scheme, when the mixture is burned in detonation waves traveling in the same (tangential) direction along the bottom of the annular channel. The detonation wave (DW) burns fresh portions of fuel mixture injected into the combustion chamber in the tail of the head wave or during its one revolution in the annular channel (in the case of a single wave). The angular frequency of rotation of the DW in a medium-size chamber is of the order of 10^5 rpm and higher.

The oxidation of fuel in the DW occurs in the mode of self-ignition at high pressures and temperatures. Therefore, the efficiency of the combustion process in the RDC, ceteris paribus, will be higher than in the LRE (the process occurs at higher pressures behind the shock wave [2]). Use of the RDC promises great benefits, at least theoretically, for the aerospace and energy industries. In particular, because the fuel burns in the RDC continuously, a turbine can be installed at the nozzle exit, on a common shaft with the compressor driving air into the annular combustion chamber. Given that the speed of the turbine is on the order of 10^4 rpm, during one revolution of the turbine, the DW makes ten or more turns, i.e., the exhaust gas flow through the crowns of the turbine can be considered nearly steady with some pulsations. In this configuration, a gas turbine with an RDC is very similar to a conventional gas turbine, but instead of continuous combustion, a DW continuously circulates in the RDC. Such a turbine, in conjunction with an electric generator, can serve as an effective stationary power plant.

To date, the greatest success in the implementation of rotating detonation has been achieved by our colleagues from the Lavrentyev Institute of Hydrodynamics of the Siberian Branch of the Russian Academy of Sciences (LIH SB RAS, Novosibirsk), F.I. Bykovsky, A.A. Vasiliev, E.F. Vedernikov, and S.A. Zhdan; a considerable contribution to solving the problem was made by deceased V.V. Mitrofanov. These researchers have conducted systematic experimental studies of continuously rotating detonation in annular

and disk combustion flow chambers of various designs with both fuel–oxygen and the fuel–air mixtures (FAMs), with gaseous and liquid fuels (see, e.g., [3–6]). Recently, these authors published the results of successful experiments on detonation combustion of wood-coal-dust–air mixtures [7]. Along with experiments, the scientists from the LIH SB RAS for the first time performed numerical simulations of the operation of the RDC, based on the equations of inviscid flow in a planar formulation with periodic boundary conditions at the ends of the interval [8]. Solving the problem by the relaxation method, the authors of [8] determined the region of existence of the detonation mode in the RDC and estimated the thrust characteristics of a jet engine on its basis.

In the past decade, interest in the RDC concept increased significantly: the works of French [9, 10], Poland [11], American [12] and Japanese [13] and Chinese [14] scientists have appeared. These papers report the results of experimental and computational-theoretical studies of the process of operation of the RDC. Experiments abroad are performed mainly with hydrogen-containing gas mixtures. As regards computational-theoretical studies, as in [8], they all are based on the equations of inviscid flow (Euler equations) for homogeneous gas mixtures.

Despite these successes, the practical application of the RDC is still discussed with great caution. The fact is that the heat flux to the walls near the nozzle head of the RDC, where detonation waves circulate, reaches enormous values. An RDC, to sustain such heating, should be made of ultra-high-temperature materials and additionally cooled. Not surprisingly that the existing laboratory RDC specimens can operate for only fractions of a second or, at best, a few seconds.

In addition to the problem of cooling, there are many other problems associated with the organization and control of the operation process. It suffices to mention only a few related physicochemical phenomena to understand the complexity of the process. To realize a stable (steady) DW circulation, it is necessary that the state of the combustible mixture before the DW front would remain unchanged or would change so little as not to affect the velocity and structure of the wave. This can be achieved only by ensuring (on the average) steady-state conditions of supply and mixing of the fuel and oxidizer, eliminating the possibility of spontaneous ignition of the fresh mixture on the hot lateral walls of the chamber near the nozzle head, and minimizing the combustion of the mixture at the developed contact boundary with the hot detonation products behind the wave front. It should be borne in mind that the tangential propagation of a DW in an annular channel of finite curvature is accompanied by diffraction effects on the outer and inner cylindrical surfaces. This leads to the formation of induced transverse-wave structures interacting with the inherent transverse waves of the detonation front. In places of collision of transverse waves belonging to different structures, areas with abnormally high pressure (which requires to substantially increase pressure in the supply lines of the nozzle head) or with reduced pressure arise. The first effect results in the penetration of the detonation products into the nozzle head, whereas the second, to the premature injection of the fuel components into the detonation products. The picture is compounded by the fact that a complete molecular mixing of the fuel components takes a finite time; i.e., a layer of mixture incapable of detonating is formed near the nozzle head. This layer is compressed and heated in an oblique shock front attached to the DW. In addition, if we take into account that the flow behind the DW is subject to a strong lateral expansion (in the direction of nozzle), it becomes clear that the flow pattern is in general unsteady and three-dimensional.

The above considerations refer to the steady-state operation of the RDC. In transient conditions, such as startup, restart, etc., the situation is more complicated. Of course, to identify the determining factors in this complex picture and to try to formulate practical recommendations, it is necessary to rely on the most advanced numerical methods for solving gas dynamics problems.

As noted above, this problem has been treated only on the basis of the inviscid flow equations. Virtually all the studies conducted so far have ignored the effects of curvature of the DW trajectory and the effects associated with the finite rate of the turbulent and molecular mixing of the fuel components with each other and with the detonation products. In such formulation of the problem, it is impossible to determine the heat fluxes to the chamber wall and their spatial distribution and to fully investigate the stability of the solution to perturbations arising upstream and downstream from the detonation region (after the compressor in the lines of supply of the combustible mixture components, at the exit of the chamber before the turbine, etc.). These effects and phenomena can become of key importance in designing the RDC for advanced jet engines and gas turbines. In particular, analysis of the molecular and turbulent transport will allow laying down requirements for the systems of supply of the fuel components and for the intensity of their mixing near the bottom of the RDC and determining the heat flux to the chamber wall. Special attention should be paid to modeling the flow near the bottom of the RDC. In the existing models, steady-state boundary conditions of consumption of the homogeneous combustible mixture are set: the consumption rate is determined by the ratio of the mixture pressure in the reservoir to the local instantaneous pressure at the bottom (with account of blocking); a negative consumption is not allowed. Obviously, in order to correctly model the flow near the bottom, it is necessary to consider the outflow of the fuel components from the correspond-

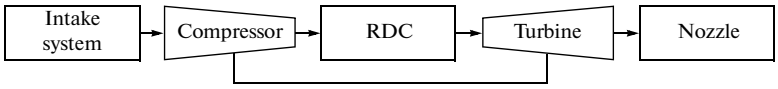

Fig. 1. Diagram of a gas turbine engine with RDC.

ing reservoirs through the openings into the combustion chamber.

The purpose of this study is to perform a three-dimensional numerical simulation of the operation of the RDC in order to determine the conditions of existence of detonation in the RDC, the thermal state of the chamber walls, and the most important parameters of the flow at the inlet and outlet of the RDC, bearing in mind the possibility of its placement between the compressor and the turbine in an advanced GTI.

GEOMETRY OF COMPUTATIONAL DOMAIN

Consider the layout scheme of a RDC-based GTI shown in Fig. 1. Such a gas turbine includes an intake system, compressor, RDC, turbine, and nozzle. The main element is an RDC in the form of a cylindrical annular combustion chamber. The air passing through the intake system and compressed in the compressor is continuously fed into the RDC, where it mixes with the fuel to form a FAM, which burns quickly in the rotating DW. The detonation products expand first in the turbine and then in the nozzle. Detonation in the RDC is accompanied by perturbations of pressure, propagating upstream and downstream. In order to attenuate these disturbances (waves), it is necessary to install gas-dynamic isolation devices (IDs) at both sides of the RDC. The corresponding IDs will be referred to as inlet (from the side of the compressor) and outlet ones (from the side of the turbine).

A diagram of an RDC with inlet and outlet IDs is shown in Fig. 2a. We made the following simplifying assumptions:

(1) the interaction of the flow in the RDC with the compressor and turbine are excluded from consideration;

(2) the RDC with height L_c, diameter phase the outer cylindrical wall d_c, and annular gap width Δ operates on a homogeneous FAM, which is fed into an annular inlet ID of height L_{ui} through the lower boundary (Fig. 2b);

(3) the static pressure P_{in} and temperature T_{in} at the lower boundary of the inlet ID are kept constant;

(4) FAM is fed into the RDC through an nozzle head in the form of two concentric annular gaps of width δ and height L_s;

(5) attached to the RDC is an annular outlet ID of height L_{di};

(6) the static pressure P_{out} at upper boundary of the outlet ID is determined by the ID volume, which is initially filled with air at a pressure of $P_{out} < P_{in}$;

(7) the temperature of all solid surfaces is kept constant, T_w.

Thus, we considered an RDC in assembly with simple annular IDs. It is understood that the level of disturbances coming from the RDC to the lower and upper boundaries of the computational domain makes it possible to judge on the maximum expected load on the compressor and turbine components, and that the heat flux to the walls of the RDC and outlet ID characterizes the worst thermal state of the walls.

Detonation in the RDC is initiated by a strong shock wave, generated in a special initiator (not shown in Fig. 2). After initiation, the DW propagates along the nozzle head, for example, counterclockwise (Fig. 2a), burning fresh FAM, while the detonation products flow from the RDC into the outlet ID and then into the turbine, predominantly in the axial direction.

The operation of the RDC under consideration is possible if a number of requirements for the chemical composition of the FAM, values of P_{in} and T_{in}, and geometric dimensions of the chamber, the nozzle head, inlet and outlet ID, material of the walls, and cooling rate are met. Generally speaking, these requirements are not known beforehand, and the region of existence of detonation in the RDC should be determined by solving the problem. Nevertheless, as a starting point for selecting the dimensions and operational parameters of the RDC, the known data on the dynamic parameters of detonation (multifront detonation cell size, critical diameter of detonation, critical thickness of semi-infinite detonating layer, etc.) and its concentration limits can be used.

MATHEMATICAL MODEL

The mathematical formulation of the problem is described in detail in [15, 16]. Here, we limited ourselves to a brief summary of its main points.

The flow of a viscous compressible gas in the computational domain was described using the three-dimensional unsteady Reynolds-averaged Navier–Stokes, energy, and species conservation equations. The turbulent fluxes of species, momentum, and energy were modeled within the framework of the standard k–ε turbulence model. Due to the above characteristics of the operation of the RDC, the contribution from the frontal combustion to the chemical sources in the equations of conservation of energy and components of the mixture was neglected. The contributions of these reactions to the indicated bulk chem-

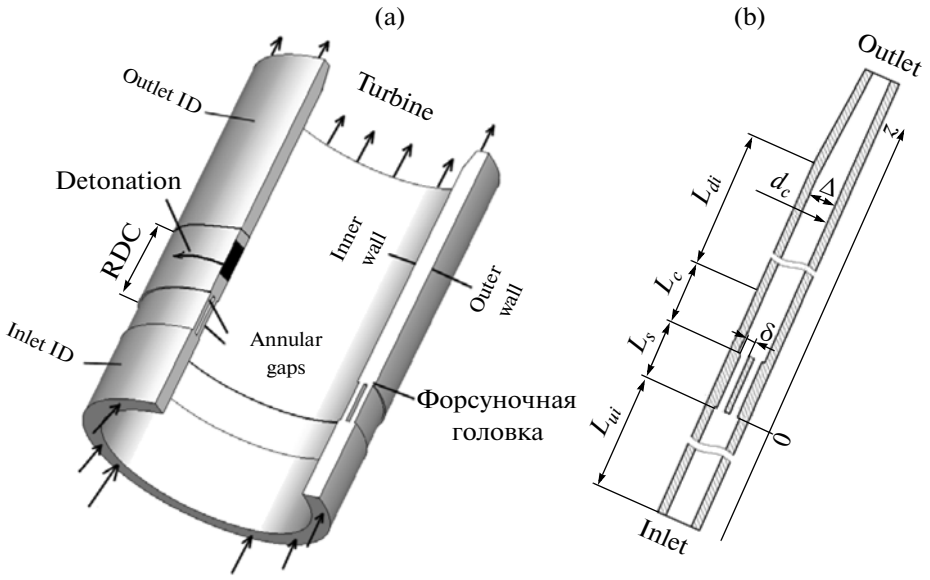

Fig. 2. (a) Rotating-detonation chamber with attached inlet and outlet isolation devices; (b) basic geometric dimensions of the chamber with longitudinal coordinate z.

ical sources were determined using the particle method (PM) [15–18].

The most important advantage of the PM is its ability to accurately determine the rates of chemical reactions in turbulent flow, without invoking any hypotheses about the influence of turbulent fluctuations on the mean rate of the reaction. In the PM algorithm, the instantaneous local states of a turbulent reacting flow are represented as a set of interacting (Lagrangian) particles. Each ith particle has its individual properties: the position in space x_k^i, three velocity components u_k^i ($k = 1, 2, 3$), volume V^i, density ρ^i, temperature T^i, mass fractions of N chemical components $y_l^i (l = 1,\ldots, N)$, and statistical weight w_i, which is used to determine the mean values of the variables over the ensemble of particles. For each ith particle, we solve the system of equations of conservation of mass of the species, momentum, and energy; the flux (transfer) terms are calculated using the classic models of linear relaxation to the mean [17].

The equations of the model were closed by the caloric and thermal equations of state of a mixture of ideal gases with variable heat capacity, as well as by the initial and boundary conditions. All the thermophysical parameters of the gas were considered variable.

METHOD OF CALCULATION AND BASIC PARAMETERS

Numerical solution of the governing equations of the problem was carried out using the dual algorithm "SIMPLE method [19]–Monte Carlo method". The chemical sources were calculated by an implicit scheme with an internal time step of integration. The dual algorithm was previously used to simulate flame acceleration and deflagration-to-detonation transition in smooth tubes and in tubes with obstacles [15, 16], as well as to solve the problems of shock-initiated autoignition and preflame ignition in confined spaces [20]. In all cases, satisfactory agreement between the results of calculations and experiments were observed.

In the present work, the FAM was a stoichiometric hydrogen–air mixture. The oxidation of hydrogen was described by a single-step reaction scheme:

$$H_2 + H_2 + O_2 \rightarrow H_2O + H_2O. \quad (1)$$

The rate of hydrogen oxidation $[\dot{H}_2]$ at elevated pressures P (5 to 40 atm) and temperatures T (1100–2000 K) was presented by the formula

$$[\dot{H}_2] = -8.0 \cdot 10^{11} P^{-1.15} [H_2]^2 [O_2] e^{-10^4/T}$$
(atm, mol, L, s).

This formula was obtained by fitting the dependences of the induction period on the pressure and temperature obtained using expression (1) to those calculated within the framework of an extensively tested detailed kinetic mechanism of hydrogen oxidation [21].

The table shows the parameters for the five variants of calculations discussed below. The values of the main parameters (in mm) of the problem were as follows:

L_{ui}	L_s	Lc	L_{di}	d_c	Δ	δ
200	50	100	450	306	23	6.9

The height of the RDC L_c was 100 mm, so that the chamber could accommodate a layer of detonating FAM of thickness approximately equal to the critical

Parameters for five calculation variants

Variant	P_{in}, atm	T_{in}, K	T_w, K	k_{in}, J/kg	ε_{in}, J/(kg s)	$Y_{H_2,in}$
1	15	293	293	10^{-3}	$2 \cdot 10^{-4}$	0.028
2	20	293	293	10^{-3}	$2 \cdot 10^{-4}$	0.028
3	10	293	293	10^{-3}	$2 \cdot 10^{-4}$	0.028
4	25	293	293	10^{-3}	$2 \cdot 10^{-4}$	0.028
5	10	580	293	10^{-3}	$2 \cdot 10^{-4}$	0.028

4 thickness [4] $h_m = (12 \pm 5)\lambda_D$, where λ_D is the multifront detonation cell width at a typical pressure in the chamber. Since the pressure in the chamber is not known beforehand, the first-guess estimate was the value of λ_D under normal initial conditions: $\lambda_D \approx 15$ mm for a stoichiometric hydrogen-air mixture at 0.1 MPa and 298 K. The values of geometric parameters d_c and Δ in the table were chosen using the experimental data from [3]. According to [4], the parameters h_m, d_c, and Δ define the total number n_D of detonation waves capable concurrently circulate in the RDC: $n_D = \pi d_a/(7 \pm 2)h_m$, where $d_a = d_c - \Delta$ is the average diameter of the chamber. It is seen that, under the selected values of $L_c \approx h_m$, d_c, and Δ, only one DW can propagate in an RDC fed with a stoichiometric hydrogen–air mixture, a result that greatly simplifies the analysis. Note, however, that these estimates are used only as a starting point for designing an RDC, whereas the actual characteristics of operation of the RDC can only be obtained by solving the problem.

The boundary conditions for the average flow velocity, pressure P, temperature T, turbulent kinetic energy k and its dissipation rate ε, and the concentrations of N chemical components Y_l ($l = 1,...,N$) on the solid walls of the computational domain were set using the formalism of wall functions on the assumption that the walls are isothermal ($T = T_w = \text{const}$), impervious, and noncatalytic, with no-slip properties. At the open boundary, from the side of the compressor, the inlet boundary conditions were specified (index "*in*") in the form of fixed values of P_{in}, T_{in}, k_{in}, ε_{in}, and $Y_{l,in}$ ($l = 1,\ldots,N$). At the open boundary from the side of the turbine (index "*out*"), a fixed value of P_{out} was set or $\partial P_{out}/\partial z = 0$. In both cases, to eliminate the influence of perturbations reflected from this open boundary on the operation of the RDC, an outlet ID of relatively large volume was attached to the RDC. In fact, the outlet ID was profiled so (Fig. 26) that the boundary condition at the given open boundary had no effect on the solution, i.e., the axial velocity component of the flow in the outlet ID would be supersonic. The other variables (velocity, temperature, turbulent kinetic energy, and its dissipation rate, as well as the concentration of the components) were extrapolated to this boundary of the computational domain. The boundary conditions for particles (components of the velocity vector and scalar variables) on the solid walls and open boundary were formulated so that they would be matched to the boundary conditions for the average values of relevant variables. This matching was continuously monitored by comparing the values of the variables obtained by averaging over the ensemble of particles in the computational cell with the average values of these variables obtained by solving the averaged equations of flow [18].

It was assumed that, at the initial time, the RDC and the inlet ID were filled with a quiescent FAM, whereas the outlet ID, with air (Fig. 3a). To initiate detonation in the RDC, we placed into the RDC a volume of finite size filled with the products of combustion of stoichiometric hydrogen–air mixture (H_2O and N_2) at elevated pressure and temperature, as shown in Fig. 3.

The initial position of the particles in the computational domain (coordinates x_k^i, $k = 1, 2, 3$) was selected using a random number generator, which provided an average uniform distribution over unit length. At the initial time, each particle had preset values of the variables u_k^i, V^i, ρ^i, T^i, y_l^i ($l = 1,\ldots,N$), and w^i, consistent with the initial distributions of the corresponding mean values. The nominal number of particles per computational cell N_p was specified before simulation. In the calculations discussed below, N_p was set equal to 10. Note that, in the course of computations, the actual number of particles in the cell could vary (particles moved over the computational domain). To keep the number of particles fixed, special procedures of cloning and clustering of particles were used [18].

To ensure the propagation of the DW in the selected direction, for example, counterclockwise in Fig. 2a, a layer of temporary inert particles was included in the initial distribution of particles in the RDC in a clockwise direction from the initiation area. Immediately after the initiation of detonation, these particles become active.

Generally speaking, the flow pattern in the RDC depended on the chosen value of N_p and on the computational grid. However, preliminary calculations showed that, at $N_p > 10$–15, the dependence of the parameters of the flow on N_p becomes weak. The calculations were performed on grids that produced no influence on such integral characteristics as the region of existence of detonation, the average static and total

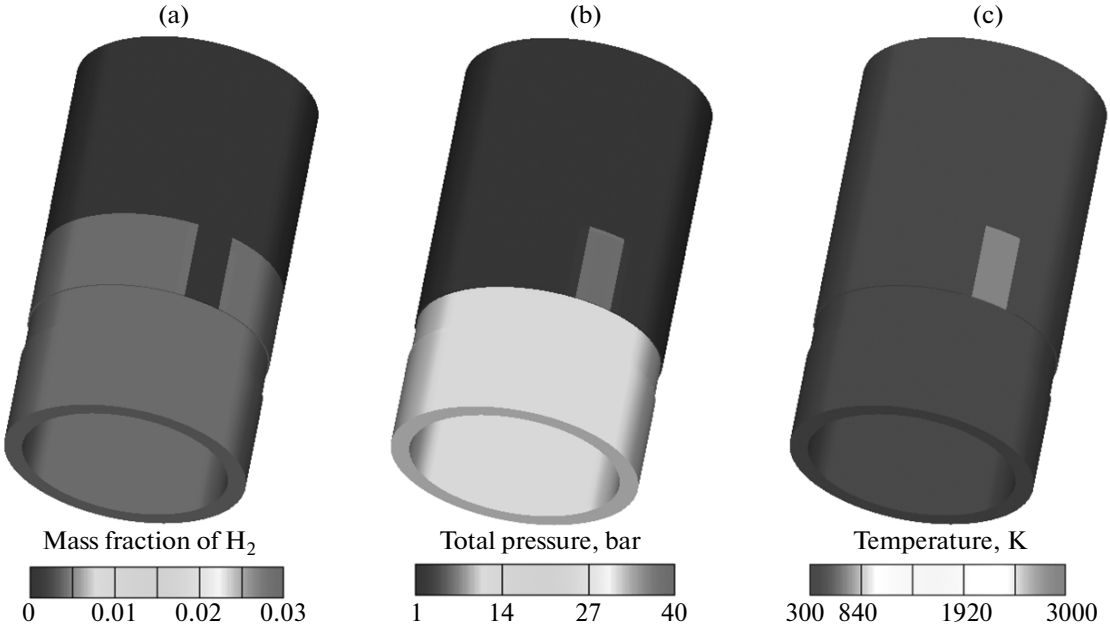

Fig. 3. Initial distributions of the (a) mass fraction of hydrogen, (b) total pressure, and (c) static temperature in the RDC with inlet and outlet IDs.

pressure in the RDC, the average heat flux to the chamber wall, and the pulsations of the flow parameters in the inlet and outlet IDs, as well as on the local characteristics, such as the velocity, curvature, and height of the DW front. As regards the internal structure of the detonation front, the grids used did not allow resolving it adequately. The last will be the subject of further studies.

SIMULATION RESULTS

Figure 4 shows the calculated distribution of the static temperature (a), total pressure (b), the mass fraction of hydrogen and heat flux to the outer wall (c) at two points in time separated by an interval of $\Delta t = 60$ μs for calculation variant 1, with $P_{in} = 1.5$ MPa. All the distributions displayed in Fig. 4 correspond to the solution in the immediate vicinity of the solid walls in the computational domain. Variant 1 predicts that only one DW circulates in the RDC, reaching the limit cycle after 3 to 4 runs of the wave around the chamber, i.e., 1–2 ms after the initiation of detonation. The rotational speed of the DW turned out to be 126000 rpm (2.1 kHz). The height of the FAM layer directly ahead of the DW (Figs. 4a, b) was ~70–80 mm, i.e., close to the critical layer thickness h_m, as estimated using the empirical criterion from [4] (despite the fact that the average static pressure in the RDC was higher than 0.1 MPa). Our attempts to simultaneously initiate two or more DW in the RDC of selected geometry failed. This result is consistent with the empirical criterion [4] for the total number n_D of DW that can simultaneously propagate in the RDC. The shock waves generated by detonation propagate upstream and downstream (Fig. 4b). The fuel burns out completely in the RDC: a small amount of unburned hydrogen in the DW (Fig. 4c) burns up in the outlet ID. Local heat fluxes to the outer wall near the nozzle head of the RDC (Fig. 4d) reach very high values, ~16 MW/m^2. It is interesting that, in one revolution of the DW, the detonation products managed to only partially penetrate into the annular gaps of the nozzle head and did not penetrate into the inlet ID at all. Note that the contribution of the dynamic component of the total pressure from the side of the compressor is relatively small (less than 3% P_{in}).

Figure 5 displays the calculated time dependences of the parameters of the process of operation of the RDC for 12 consecutive revolutions of the DW, starting with the initiation of detonation. The dependences are shown for the static pressure P (Fig. 5a) and the static temperature T (Fig. 5b) at a point located at a distance of $z = 20$ mm from the nozzle head at the center of the gap of width Δ. For comparison, Fig. 5 shows two families of curves: for calculation variant 1 (solid curves) and variant 2 (dashed lines). The horizontal dotted lines in Fig. 5a correspond to the mean static pressure, as obtained by averaging over the RDC volume after the limit cycle was reached in both calculation variants. As can be seen, the average static pressure in the RDC depends on P_{in}: the higher the P_{in}, the greater the pressure in the RDC. The obtained values of the mean static pressure (1.44 and 1.94 MPa) turned out to be slightly lower (by 4% and 3%) than the corresponding values of P_{in}. However, the values of total pressure, obtained by averaging over the RDC volume

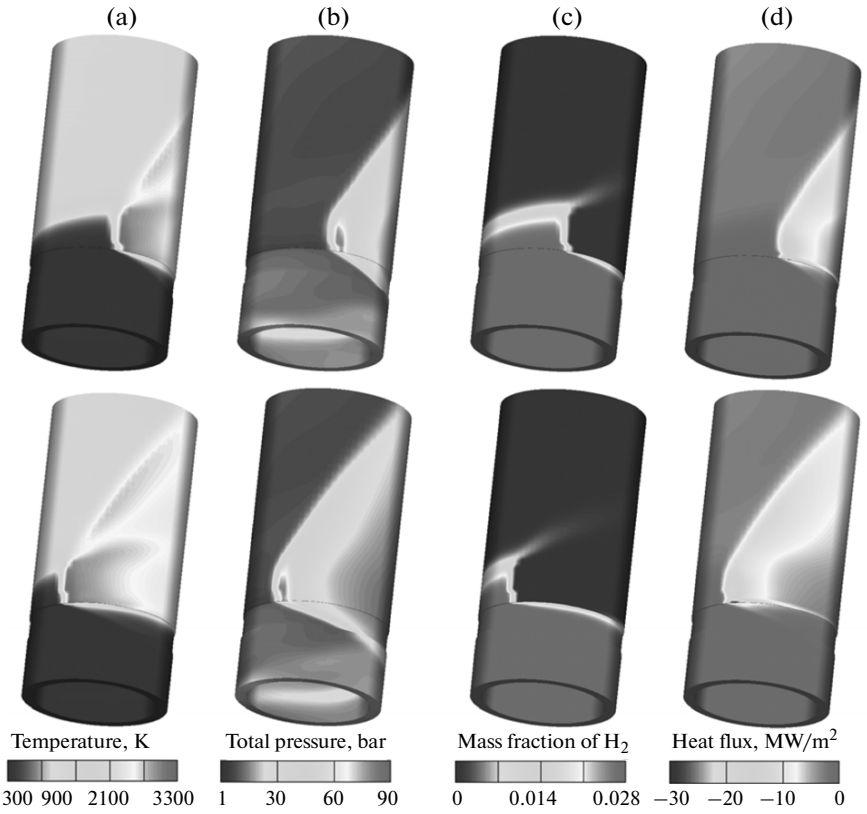

Fig. 4. Calculated distributions of the (a) static temperature, (b) total pressure, (c) mass fraction of hydrogen, and (d) and heat flux to the walls at times $t = 5.75$ ms (top) and 5.84 ms (bottom) for variant 1.

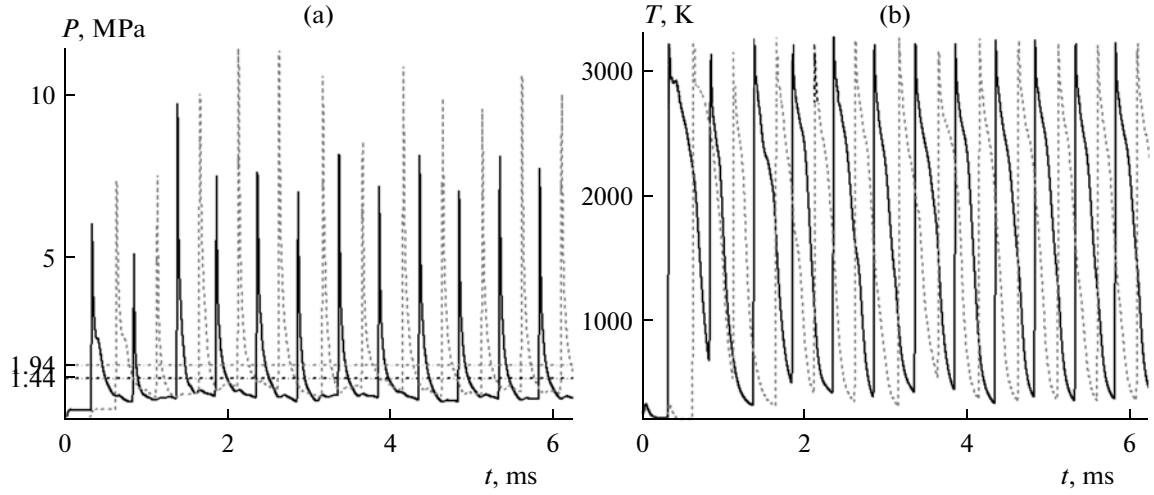

Fig. 5. Calculated time dependences of the (a) static pressure and (b) static temperature in the RDC at a distance of $z = 20$ mm from the nozzle head at the center of the gap for variants 1 (solid curves) and 2 (dashed). The dotted line shows the static pressure obtained by averaging over the RDC volume upon the onset of limit cycle.

after reaching the limit cycle were higher than P_{in}, 1.71 and 2.35 MPa for variants 1 and 2, respectively. This means that the total pressure in the RDC increases by about 11% P_{in} and 14% P_{in}, respectively. The total pressure in the RDC increases despite the fact that the energy release occurs in a relatively narrow (70–80 mm) layer of FAM, limited by external and internal walls of the chamber, partially limited (with a permeability of 0.6) by the nozzle head, and is not limited whatsoever from the side of the turbine. That is why the RDC is often referred to as a combustion chamber with pressure increase. In contrast to the static pressure, the static

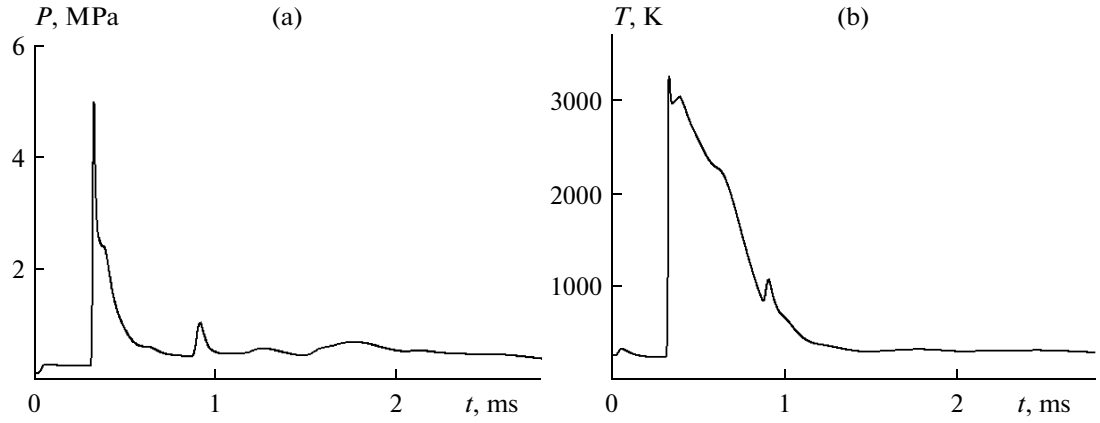

Fig. 6. Calculated time evolution of the (a) static pressure and (b) static temperature at a point located at the center of the gap at a distance of $z = 20$ mm from the nozzle for variant 3 with detonation failure.

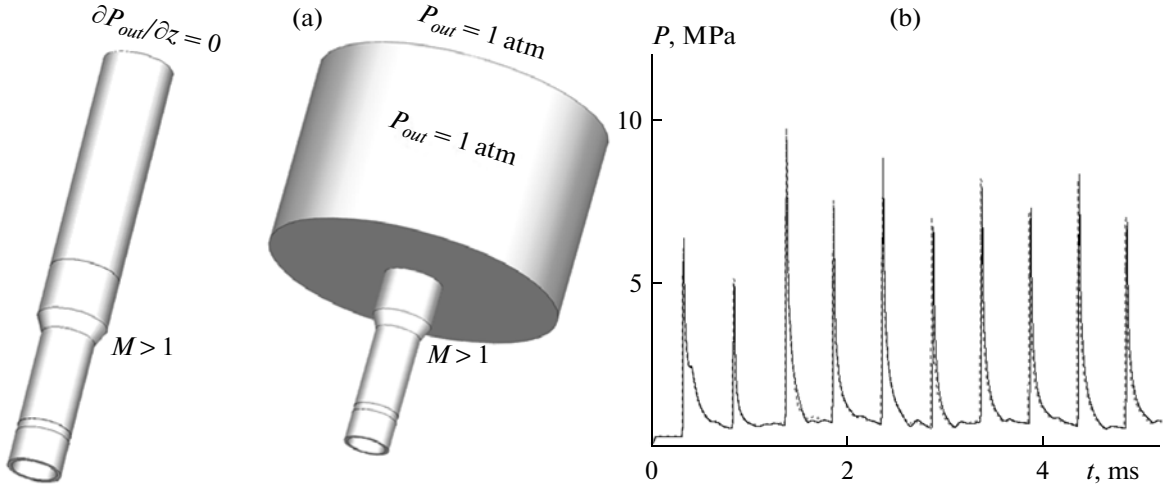

Fig. 7 (a) Various boundary conditions at the outlet of the computational domain; (b) the calculated time dependences of the static pressure a point located at a distance $z = 20$ mm from the nozzle head for various boundary condition: $P_{out} = 0.1$ MPa (solid line) and $\partial P_{out}/\partial z = 0$ (dashed line).

temperature is practically independent of P_{in} (Fig. 5b). The mean detonation velocity in both variants was ~1850 m/s, which is 6% lower than the Chapman–Jouguet detonation velocity for a stoichiometric hydrogen–air mixture under normal initial conditions (~1970 m/s).

Our attempts to obtain a stable operation at $P_{in} <$ 1.3 MPa and $P_{in} > 2.5$ MPa, with the other conditions corresponding to variants 1–3, were not successful. For example, at $P_{in} = 1.0$ MPa, after initiation, detonation decayed (Fig. 6). At $P_{in} > 2.5$ MPa, detonation failure was caused by a very large flow rate of FAM through the nozzle head: the reaction zone was displaced from RDC. In addition, in these conditions, due to the rapid mixing of fresh mixture with detonation products, ignition kernels arose, which violated the homogeneity of the gas behind the DW. Thus, detonation in the RDC of chosen geometry occurred only within a range of $1.3 \le P_{in} \le 2.5$ MPa.

Figure 7 shows the variations of the boundary conditions from the side of the turbine (Fig. 7a) do not affect the operation of the RDC. Indeed, the calculated time dependences of the mean static pressure (and the other averaged parameters of the flow) at any point in the RDC remained unchanged regardless of what boundary conditions were set at the upper boundary of the outlet ID, be it $P_{out} = 0.1$ MPa or the absence of the axial pressure gradient, $\partial P_{out}/\partial z = 0$ (Fig. 7b).

Figure 8a shows another important feature of the flow in the vicinity of the nozzle head of the RDC, namely a difference between the maximum static pressure at the inner and outer cylindrical walls of the chamber. The solid and dashed curves in Fig. 8a show the calculated time evolution of the static pressure at the inner and outer walls of the chamber for two operation cycles. Due to the diffraction of the DW, the maximum pressure at the outer wall is 20–25% higher

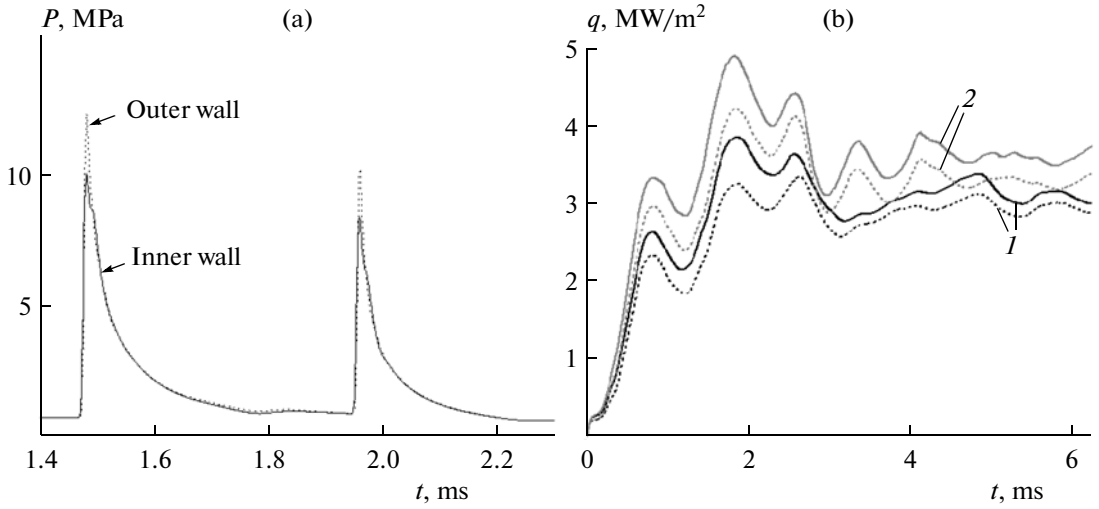

Fig. 8. (a) Calculated time histories of the static pressure at the inner (solid line) and outer (dashed line) walls of the RDC in a section located near the nozzle head for variant 1; (b) time histories of the total heat flux at the inner (dashed curves) and outer walls (dashed) of the RDC and attached outlet ID for variants 1 (curves *1*) and 2 (curves *2*).

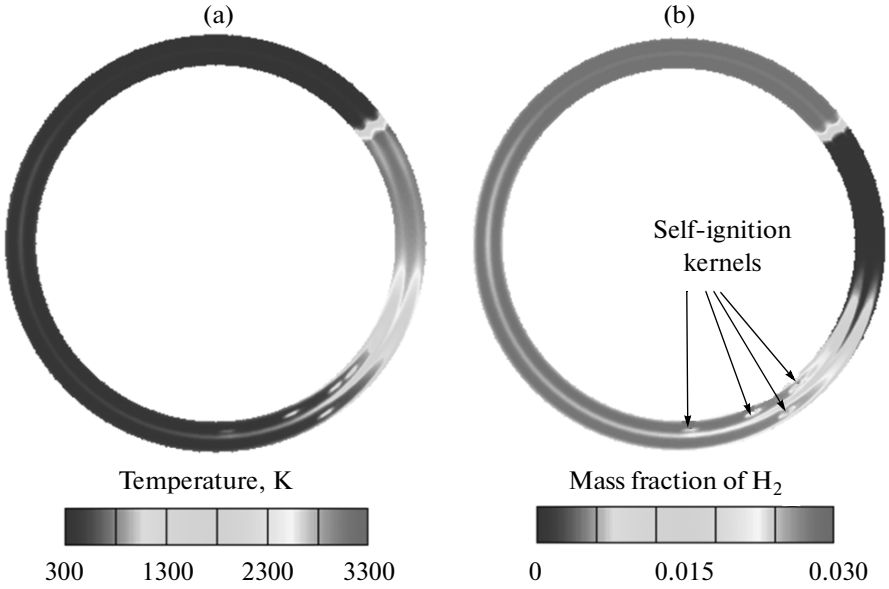

Fig. 9. Calculated distribution of the (a) static temperature and (b) mass fraction of hydrogen in the RDC in section $z = 5$ mm above the nozzle head in variant 4.

than at the inner wall, but otherwise, the curves are practically identical.

Figure 8b displays the calculated dependence of the total heat flux to the inner (solid lines) and outer (dashed lines) walls of the RDC with the outlet ID attached for variants 1 (curve *1*) and 2 (curves *2*). The total heat flux was calculated as the average integral value over the surface area of the interior or exterior walls. It is seen that the heat flux to the inner wall is higher than that to the outer. In calculation variant 1, this difference amounted to 5%, whereas for variant 2, to 10%. With increasing P_{in}, the heat flux to the walls increased: in variants 1 and 2, the calculated average values of the total heat flux to both the wall were ~3 and 2.0–3.5 MW/m^2, respectively.

Figure 9 shows the calculated distributions of the static temperature and mass fraction of hydrogen in a section of the RDC located at a height of $z = 5$ mm above the nozzle head for variant 4 with $P_{in} = 2.5$ MPa (table). As can be seen, the mixture ahead of the DW traveling in a counterclockwise direction is nonuniform in temperature and composition. As a consequence, the detonation front becomes W-shaped, with the leading points located at the inner and outer walls, as well as at the center of the gap. Another important feature of the flow is the formation of ignition kernels

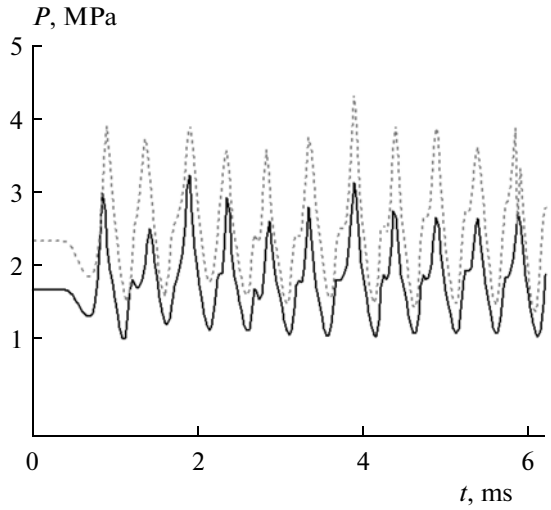

Fig. 10. Calculated time dependences of the static pressure at a point in the inlet ID at $z = 150$ mm for variants 1 (solid curves) and 2 (dashed).

behind the DW. These kernels arise due to a rapid mixing of inflowing fresh mixture with hot detonation products.

Of considerable practical interest are the flow characteristics in the inlet and outlet IDs, from side of the compressor and turbine, respectively. Figure 10 shows the calculated time dependences of the static pressure in the inlet ID in a section with $z = -450$ mm for variants 1 (solid line) and 2 (dashed line).

We see that the pressure pulsations in the inlet ID reach (40÷45%) P_{in}. Such pulsations cause local changes in the direction of flow (gas velocity at the entrance to the ID becomes negative), a highly undesirable effect. Thus, to prevent the unstable operation of the compressor, pressure pulsations should be damped. Note that, in calculations, the particles in the inlet ID were considered inert. This was done, firstly, to prevent the penetration of detonation into the ID and, secondly, to model an actual process with independent air supply (through the inlet ID) and hydrogen (directly into the nozzle head).

Figure 11 presents the calculated time evolution of the static pressure (Fig. 11a) and static temperature (Fig. 11b) at a point in the outlet ID with $z = 475$ mm for variants 1 (solid curves) and 2 (dashed curves). It is seen that the annular outlet ID, which is a simple extension of the RDC reduces the amplitude of pulsations of the static pressure and static temperature as compared to similar pulsations near the nozzle head (Fig. 5). Nevertheless, the absolute values of pressure fluctuations are sufficiently large: ±0.5 MPa at $P_{in} =$ 1.5 MPa and ±0.7 MPa at $P_{in} = 2.0$ MPa, i.e., at a level of (30÷35%) P_{in}. The corresponding macroscopic (nonturbulent) fluctuations of static temperature reach ±250 K at 2500 K, i.e., ~10%. Obviously, the outlet ID must be designed in such a way as to damp pressure and temperature pulsations. Moreover, the average temperature of detonation products (~2500 K) is too high for the turbine. Therefore, to reduce the temperature at the gas turbine inlet, the RDC should operate on fuel-lean mixtures or the outlet ID should be equipped with special holes for admixing relatively cold secondary air.

Figure 12a illustrates a simple example with an outlet ID equipped with three radial holes 5 mm wide, which connect the ID with an additional annular air-cooling circuit. As shown in Fig. 12a, air is driven through the additional circuit. Figure 12b compares the calculated time evolution of the static temperature under conditions of variant 1 at the same point as in Fig. 11 without (solid curve) and with (dashed line) air cooling. It is seen that admixing of air to in the detonation products makes it possible to reduce the average static temperature and the amplitude of its pulsations in the outlet ID. By contrast, the average static pressure in the RDC increases due to admixing secondary air (Fig. 12c). This is consistent with the experimental observations reported in [3]. Note that according to [3], admixing of air to detonation products increases the specific impulse per fuel consumed and, therefore, decreases specific fuel consumption. However, this is beyond the scope of this article.

So far we have considered variants with supply of a cold FAM into the RDC ($T_{in} = 293$ K). In reality, in the inlet ID of a gas turbine, the air is heated due to compression in the compressor to the pressure P_{in}. Figure 13 shows the results of calculations for variant 5, in which the temperature of the FAM at the entrance to the computational domain was $T_{in} = 580$ K, with the geometry of the computational domain being the same as in Fig. 2. It displays the time dependences of the static pressure (Fig. 13a) and total heat flux to the walls of the RDC and attached outlet ID (Fig. 13b). In this case, the operation of the RDC at $P_{in} = 1.0$ MPa was

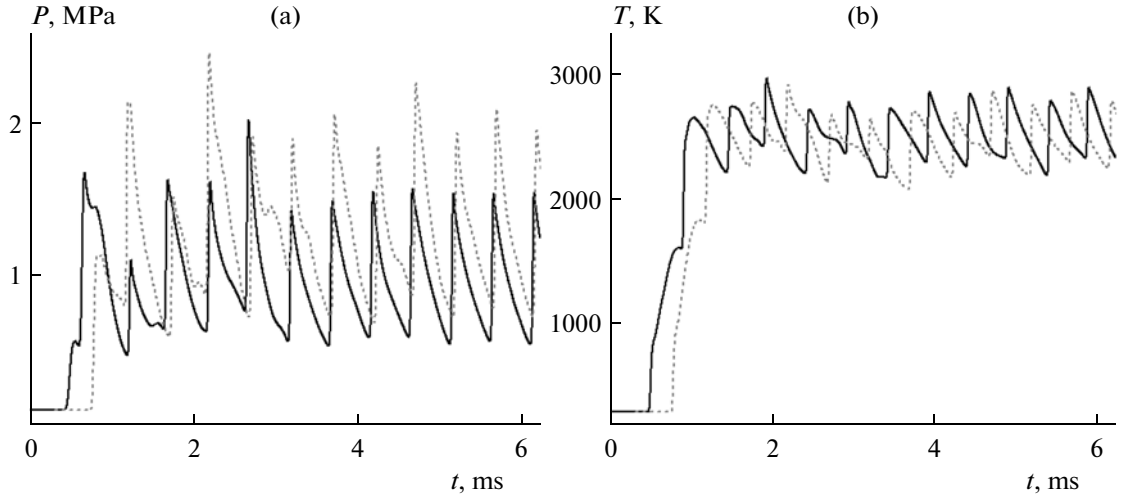

Fig. 11. Calculated time dependences of the (a) static pressure and (b) static temperature at a point in the outlet ID at $z = 475$ mm for variants 1 (solid curves) and 2 (dashed).

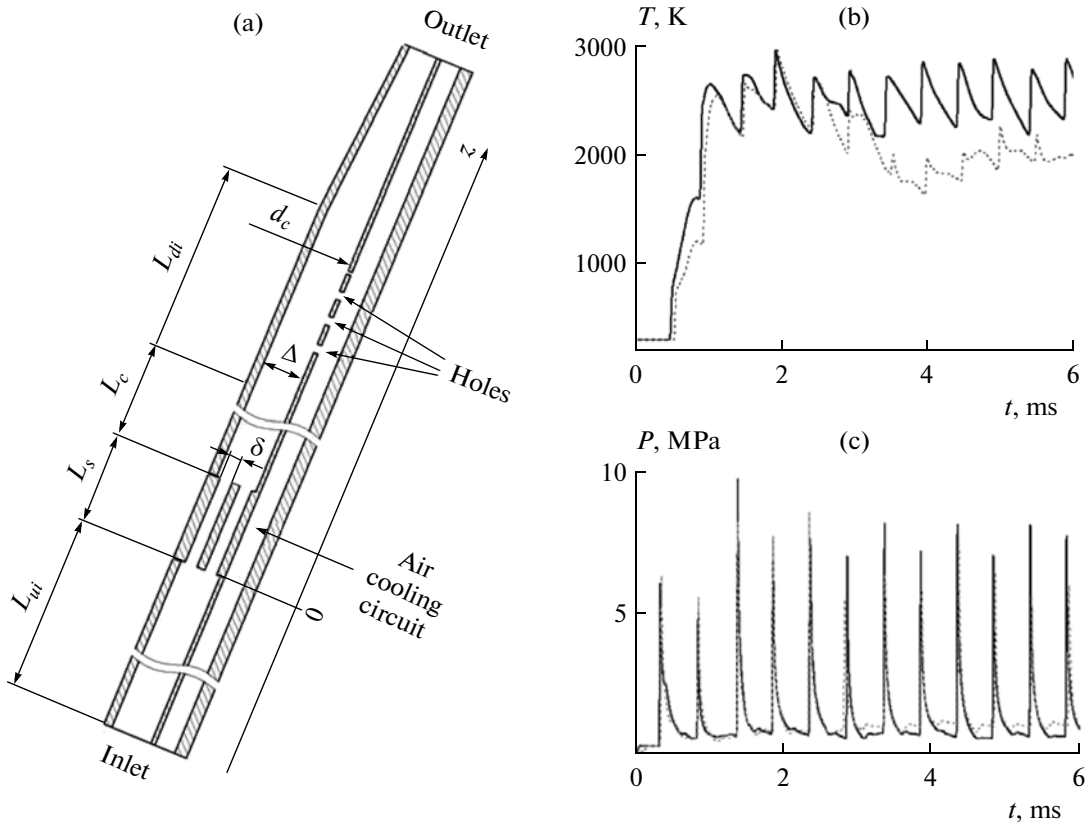

Fig. 12. (a) Diagram of an RDC with inlet and outlet IDs and with an additional annular air-cooling circuit; calculated time dependence of the (b) static temperature and (c) static pressure without (solid curves) and with (dashed curves) the cooling circuit at $P_{in} = 1.5$ MPa.

stable, which was impossible at $T_{in} = 293$ K. The static pressure obtained by averaging over the volume of the RDC (0.93 MPa) and the amplitude of pressure peaks (≈4 MPa) in the RDC was lower as compared with those in variant 1. The total pressure averaged over the RDC volume was also lower, 1.08 MPa. The total heat

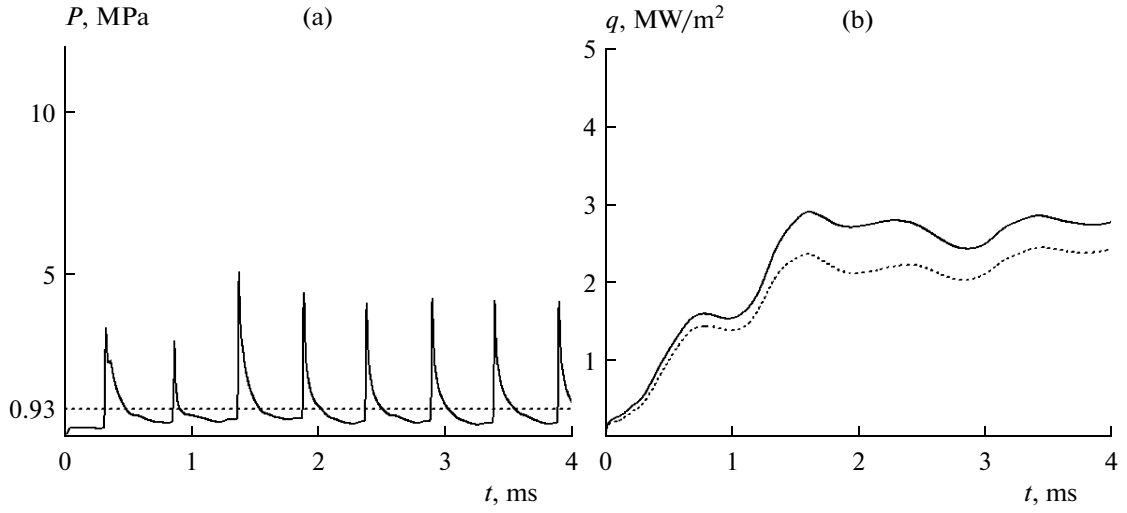

Fig. 13. Calculated time evolution of the (a) static pressure and (b) total heat flux to the inner (solid curve) and outer (dashed) walls of the RDC and outlet ID for variant 5 (P_{in} = 1.0 MPa and T_{in} = 580 K). In case a, the dotted curve represents the static pressure average over the RDC volume upon the onset of the limit cycle.

flux to the walls of the RDC and outlet ID decreased approximately to 2.5 MW/m^2. As for the amplitude of pressure pulsations in the IDs, it remained at the same level: (40÷45%) P_{in} for the inlet ID and (30÷35%) P_{in} for the outlet ID.

CONCLUSIONS

Thus, we have developed a computer program that makes it possible to perform full-scale three-dimensional simulations of the operation of the rotating-detonation chamber. As an example, an annular combustion chamber operating on a stoichiometric hydrogen–air mixture was considered.

It was shown that, for the chosen configuration of the RDC, a steady operation is possible with one DW rotating above the nozzle head at a frequency of 126000 rpm (2.1 kHz). The region of existence of detonation in the RDC is limited to the range $1.3 \le P_{in} \le 2.5$ MPa (at T_{in} = 293). Since the temperature T_{in} increases due to adiabatic compression in the compressor, the lower boundary of existence of detonation in the RDC lowers to $P_{in} \approx 1.0$ MPa. In all calculation variants providing stable operation, the total pressure in the RDC was higher than P_{in}, a result that confirms the fact that the RDC is a combustion chamber with pressure increase.

In the course of simulation, special attention was paid to the characteristics of flow in the inlet and outlet IDs, which are supposed to communicate with the compressor and turbine. We considered IDs of the simplest annular shape. It was assumed the level of disturbances coming from the RDC to the lower and upper boundaries of the computational domain will allow evaluating the maximum expected load on the compressor and turbine components, whereas the heat fluxes to the walls of the RDC and outlet ID will provide information on the worst thermal state of the walls. The temperature of the detonation products in the outlet ID turned out to be ~2500 K. To reduce the gas temperature before the turbine, we propose to dilute detonation products with secondary cold air coming into the outlet ID through radial openings. It is shown that this method makes it possible to reduce the mean static temperature and the amplitude of its fluctuations in the outlet ID.

Calculations have shown that the amplitude of pressure fluctuations in the inlet and outlet IDs can reach very high values (40÷45%) P_{in} and (30÷35%) P_{in}, respectively. The amplitude of pulsations of the average static temperature in the outlet ID can reach 10% of the mean level. Thus, to eliminate unwanted mechanical load on the compressor and turbine components and to exclude dangerous off-nominal modes of operation (such as compressor surge), it is necessary to take special measures to dampen such pulsations.

The local and total heat fluxes to the wall of the RDC and outlet ID were calculated. It was shown that local heat fluxes near the nozzle head could be as high as 16 MW/m^2; however, the total heat flux, defined as the integral average heat flux at the inner and outer walls of the RDC and outlet ID, was at a level of 2.5–3.5 MW/m^2, depending on the pressure of FAM supply.

ACKNOWLEDGMENTS

This work was supported by the Russian Foundation for Basic Research, project no. 11-08-01297.

REFERENCES

1. B. V. Voitsekhovskii, Dokl. Akad. Nauk SSSR **129**, 1254 (1959).

2. Ya. B. Zel'dovich, Zh. Tekh. Fiz. **10**, 1453 (1940).
3. F. A. Bykovskii, S. A. Zhdan, and E. F. Vedernikov, Combust. Explos., Shock Waves **46**, 52 (2010).
4. F. A. Bykovskii, S. A. Zhdan, and E. F. Vedernikov, J. Propuls. Power **22**, 1204 (2006).
5. F. A. Bykovskii, S. A. Zhdan, and E. F. Vedernikov, Fiz. Goreniya Vzryva **41** (4), 99 (2005).
6. F. A. Bykovskii, S. A. Zhdan, and E. F. Vedernikov, Dokl. Phys. **54**, 29 (2009).
7. F. A. Bykovskii, S. A. Zhdan, E. F. Vedernikov, and Yu. A. Zholobov, Dokl. Phys. **55**, 142 (2010).
8. F. A. Bykovskii, S. A. Zhdan, and E. F. Vedernikov, Combust. Explos., Shock Waves **45**, 606 (2009).
9. D. M. Davidenko, I. Gokalp, and A. N. Kudryavtsev, in *Deflagrative and Detonative Combustion,* Ed. by G. D. Roy and S. M. Frolov (Torus Press, Moscow, 2010), p. 27.
10. D. M. Davidenko, I. Gokalp, and A. N. Kudryavtsev, AIAA Paper No. 2008-2680 (2008).
11. J. Kindracki, P. Wolanski, and Z. Gut, Shock Waves **21** (2), 75 (2011).
12. D. A. Schwer and K. Kailasanath, Proc. Combust. Inst. **33** (2010, in press); http://www.sciencedirect.com/science/article/pii/S1540748910003159.
13. M. Hishida, T. Fujiwara, and P. Wolanski, Shock Waves **19** (1), 1 (2009).
14. Ye-Tao Shao, Meng Liu, and Jian-Ping Wang, Combust. Sci. Technol. **182**, 1586 (2010).
15. V. S. Ivanov and S. M. Frolov, Russ. J. Phys. Chem. B **4**, 597 (2011).
16. S. M. Frolov and V. S. Ivanov, in *Deflagrative and Detonative Combustion*, Ed. by G. D. Roy and S. M. Frolov (Torus Press, Moscow, 2010), p. 133.
17. S. B. Pope, Prog. Energy Combust. Sci. **11**, 119 (1985).
18. S. M. Frolov, V. Ya. Basevich, M. G. Neuhaus, and R. Tatschl, in *Advanced Computation and Analysis of Combustion*, Ed. by G. D. Roy, S. M. Frolov, and P. Givi (ENAS Publ., Moscow, 1997), p 537.
19. S. Patankar, *Numerical Methods of Solution of Problems of Heat Transfer and Dynamics of Liquid* (Energoatomizdat, Moscow, 1984) [in Russian].
20. S. M. Frolov, in *Teaching Materials for the 4th European Summer School on Hydrogen Safety, Sept. 7–16, 2009, Corsica, France*, Paper No. 12.
21. V. Ya. Basevich and S. M. Frolov, Usp. Khim. **76**, 927 (2007).

SPELL: 1. ceteris, 2. paribus, 3. inviscid, 4. multifront, 5. deflagration